Review

Qunshuo Wei, Lingling Huang*, Thomas Zentgraf and Yongtian Wang

Optical wavefront shaping based on functional metasurfaces

https://doi.org/10.1515/nanoph-2019-0478
Received November 25, 2019; revised January 3, 2020; accepted January 7, 2020

Abstract: Regarded as a kind of smart surfaces, metasurfaces can arbitrarily tailor the amplitude, phase, and polarization of light. Metasurfaces usually consist of subwavelength nanoantenna or nanoresonator arrays, which are delicately designed and processed. As an ultrathin, miniaturized versatile wavefront modulation device, metasurfaces have great information capacity and can arouse the future development of highly integrated micro-nano optoelectronic systems. Exploiting the advantages of ultrasmall pixels, flexible design freedom, low loss, and easy processing properties, metasurfaces provide potential feasibility and new perspectives for a plethora of applications. Here we review the research progress of metasurfaces for holographic displays, polarization conversion, active modulation, linear and nonlinear wavefront modulation, and prospect the future development trend of metasurfaces.

Keywords: metasurface; holographic display; wavefront modulation; polarization conversion; active modulation; nonlinear wavefront modulation.

1 Introduction

Metasurfaces have attracted extensive attention and became a rapidly developing research field due to their unique abilities of arbitrarily modulating the phase, amplitude, and polarization of the electromagnetic wave with compact footprint and powerful versatility of producing various special optical effects [1–6]. Metasurfaces usually consist of periodic, quasi-periodic, or randomly arranged subwavelength antenna arrays, which are made of metal or dielectric structures with specific geometries. Their wavefront modulation mechanism does not rely on the accumulation effect during the light propagation process, but by elaborately designing the geometry shapes, structural sizes, and spatial orientation angles of the nanoantennas, utilizing their strong interaction to the incident light field to realize the abrupt phase, amplitude change, and other parameters' modulation. Compared with traditional optical components and bulk metamaterials, metasurfaces benefit from the reduced absorption loss; relatively low fabrication difficulty; ultrathin, ultrasmall pixel size; and broadband characteristics. They can effectively reduce the size of the devices and have significant advantages in the integration with on-chip nanophotonic devices. Due to their great flexibilities, metasurfaces provide a new perspective for the design of various optical systems. Metasurfaces have great potential in plethora of applications such as holography [7–9], generation of vortex beam [10–12], data storage [13, 14], encryption and anticounterfeiting [15, 16], metalens and dispersion control [17–19], asymmetric transmission [20–22] and nonlinear optics [23–27], and so on, and draw a grand blueprint for the development of optical components to miniaturization, integration, and multifunction.

The wavefront modulation mechanisms of metasurfaces are basically based on three kinds of representative design methods: (1) optical resonance from nanoantennas: by adjusting the geometric parameters such as the size and orientation angle of each optical antenna, the properties of the radiation wave can be modulated. Typical structures include V-shaped antennas [28], Y-shaped antennas [29], C-shaped antennas, and so on. (2) Huygens' metasurfaces: by matching the electric and magnetic polarizability within the nanostructure, the transmission can reach unity, and the building block can be viewed as secondary wave sources. This design method was first experimentally verified in the microwave band [30], and then the dielectric Huygens' metasurfaces, which are applied in the holographic field, were also reported [31, 32]. (3) Pancharatnam–Berry (PB) phase (also known as geometric

***Corresponding author: Lingling Huang,** School of Optics and Photonics, Beijing Institute of Technology, Beijing 100081, China, e-mail: huanglingling@bit.edu.cn. https://orcid.org/0000-0002-3647-2128
Qunshuo Wei and Yongtian Wang: School of Optics and Photonics, Beijing Institute of Technology, Beijing 100081, China
Thomas Zentgraf: Department of Physics, Paderborn University, Warburger Straße 100, 33098 Paderborn, Germany

phase), which can be achieved by spatially rotating the nanoantennas: the incident lights of the same polarization state will produce different phase changes when they reach the same final polarization state through different paths on the Poincaré sphere. The phase change has pure geometric property, so it is wavelength independent.

With the advancement of metasurfaces and nanofabrication technology, the focus and emphasis of research have been pushed forward from principles to applications. Large information capacity and multifunctionality become the research focus for metasurfaces. Except for various multiplexing technologies for static metasurfaces, another intriguing method is to use phase-change materials or other ways to modulate the characteristics of electromagnetic waves based on metasurfaces through external stimuli such as light, heat, electricity, magnetism, and force. These reconfigurable metasurfaces can avoid the obstruction of the material characteristics and fixed structures. In addition, the nonlinear effect, which is aroused by the interaction between the strong laser (such as femtosecond laser pulse) and the metasurfaces, leads to the information modulation at newly generated frequencies. According to the selected optical nanoantennas with different shapes, sizes, material components, and different wavefront modulation mechanisms, the phase, amplitude, polarization, angular momentum, frequency, and dispersion can be controlled by metasurfaces; many unique optical properties such as designable spectral responses, dynamic switching characteristics, and nonlinear harmonic generation characteristics can be realized.

In this review, we briefly discuss the research progress of metasurfaces in the fields of holographic display, wavefront modulation, and polarization conversion in recent years. Next, some novel directions such as active reconfigurable metasurfaces and nonlinear metasurfaces are introduced. Finally, we also propose the expectations and potential development directions of metasurfaces.

2 Metasurface holography

Holography refers to the optical technique for controlling the wavefront of light as desired by spatially varied phase and amplitude. Holograms do not record an image directly, but record a series of amplitude and phase distributions that appear "random distributions." Because a hologram contains the complete information of the target object's scattered wavefront, it can effectively reconstruct the depth information and provide a vivid three-dimensional (3D) observation to human eyes. Due to this unique advantage compared with other display technologies, holography is considered as the ultimate 3D display scheme. In recent years, the holographic technology has made great progress and has been widely used in many applications such as stereo display, interferometry, data storage, medical imaging, remote sensing imaging, image processing, and recognition. Notably, one of the cut-in-edge research is the combination of holography principle and metasurfaces, that is, encoding the amplitude and phase distributions of holograms with two-dimensional arrays of subwavelength antennas. Compared with the traditional holographic display technology based on the spatial light modulator, metaholograms not only keep the ultrathin and compact characteristics of metasurfaces, but also overcome many challenges faced by the traditional holography, such as multiple diffraction orders, small field of view, narrow bandwidth, twin image, and so on, which greatly improve the reconstruction quality.

In general, the first step of designing a metahologram is to numerically calculate the phase and amplitude distributions on the hologram plane using computer-generated holography (CGH) algorithms. The diffraction patterns can be expressed by the Fresnel–Kirchhoff integral [33, 34]:

$$U_h(x, y, z) = \frac{1}{j\lambda}\iint U_0(x_0, y_0, z_0)\frac{\exp(jkr)}{r}dx_0dy_0 \tag{1}$$

where $U_0(x_0, y_0, z_0)$ and $U_h(x, y, z)$ represent the complex amplitude on the object plane (x_0, y_0, z_0) and the hologram plane (x, y, z), respectively; k indicates the wave vector; and the distance between two points on the object plane and the hologram plane is $r = \sqrt{(x_0 - x)^2 + (y_0 - y)^2 + (z_0 - z)^2}$. According to the above formula, one can simulate the propagation of light and directly calculate the complex amplitude $U_h(x, y, z)$ of the hologram plane. Note different algorithms have been proposed for adapting to different types of metasurfaces [35, 36], including point sources method, angular spectrum method, and iterative Fourier transform algorithm such as Gerchberg–Saxton algorithm.

In order to fully utilizing the excellent wavefront modulation ability and flexible design freedom of metasurfaces, various schemes for holographic display based on different methods have been proposed in succession [37–39]. Among the wavefront modulation mechanisms, PB phase modulation method has broadband dispersionless characteristics; the phase of each nanoantenna is related to the combination of the incident and output polarization states and can be modulated continuously without affecting the amplitude. The design of the nanoantennas for PB phase metasurfaces is relatively simple. Different structures, including rods, coupled dimers, metal–dielectric–metal structure, rectangular/elliptical

columns, and so on, can be used to build up a PB phase metasurface. Taking the metal rod nanoantenna as an example, by rotating the orientation angles of the nanoantennas, the local phase information can be easily encoded, and then the required phase distribution of a CGH can be achieved [35]. In the experiment, for a certain circularly polarized incident light, the target image can be obtained by taking the output circularly polarized light with opposite helicity. This method can effectively increase the field of view of 3D holography, realize the coaxial reconstruction of the holographic image, and avoid higher-order diffractions. In contrast, due to the lack of independent control of the amplitude and phase, the metaholograms that rely on the resonant response of the nanoantennas have to carefully design their structural parameters and need complex micronano processing technology.

For metaholograms, information capacity is a very important indicator. In order to improve the information capacity of a metahologram, the concept of holographic multiplexing was proposed, which means recording two or more images simultaneously in a single metasurface without increasing the number of pixels. At present, the representative metasurface holographic multiplexing technologies include synthetic spectra method, spatial multiplexing, polarization multiplexing [40], wavelength multiplexing [41, 42], and angle multiplexing [43]. In addition, there are also some distinctive holographic multiplexing methods such as polarization and frequency multiplexed by C-shape bar resonators [44], spatial frequency multiplexing [45], orbital angular momentum (OAM) multiplexing [46], and so on. These above methods achieve holographic multiplexing by using special algorithms and wavefront modulation mechanisms, constructing new coding units, introducing new degrees of freedom, or increasing the complexity of nanoantennas. Hence, metasurface becomes a platform of high-capacity holographic display and data storage system with low cost and high performance.

One kind of commonly used holographic multiplexing method is to directly space and interleave two groups of nanoantennas that correspond to different wavefronts to synthesize a hybrid hologram. For example, two groups of mutually orthogonal nanoantennas can be used for holographic multiplexing based on the linear polarization selectivity [47], and two groups of interleaved nanoantennas under circularly polarized light illumination can be used for PB phase multiplexing [48]. These metaholograms based on spatial multiplexing methods are intuitive and easy to design. However, these approaches can reconstruct only a few images, and the available spatial bandwidth product of each subhologram is inevitably reduced; the increase of information capacity is limited. In order to further improve the information capacity of

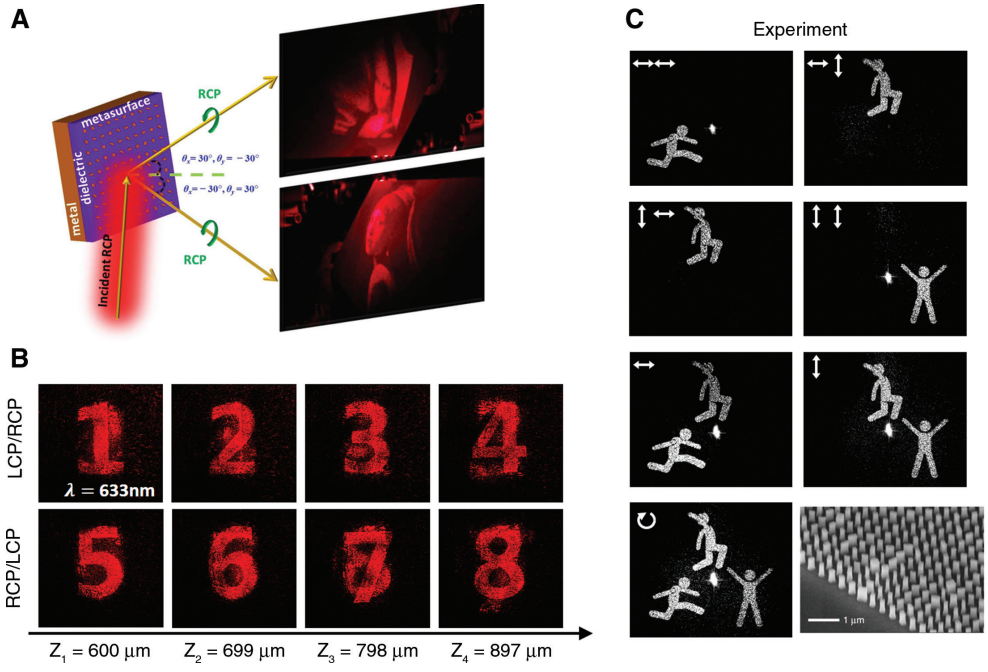

Figure 1: The holographic multiplexing of metasurfaces.
(A) Schematic diagram of hybrid holographic multiplexing metasurface [49]. (B) Experimental results of broadband multiplane metasurface hologram based on the 3D Fienup algorithm [36]. (C) Experimental results of full vectorial metasurface hologram with different polarization combinations [50].

holograms, the synthetic spectra method was proposed [49], as shown in Figure 1A. By linearly combining the individual hologram spectra of various objects with different phase shifts, the total complex amplitude of the synthetic hologram can be obtained. Utilizing the helicity-dependent characteristic of the PB phase metasurfaces and integrating polarization, position, and angle parameters together as the unique reconstruction key for each primary image, hybrid holographic multiplexing schemes were achieved. To further improve the transmission efficiency of the metasurface, plasmonic coupled dimers and reflective metal–insulator–metal structure or dielectric resonators are proposed as the building blocks of metasurfaces. For example, coupled dimers can exhibit large field enhancement in their small gap regions. Compared with the ordinary metal nanorods, they can increase the polarization conversion by about 50%. Meanwhile, a 3D-Fienup algorithm was proposed to achieve the phase retrieval of the CGH, which contains all the information of multiple images at different reconstruction planes [36]. As shown in Figure 1B, two multiplexing methods, position multiplexing and polarization multiplexing, were integrated so as to obtain the ability to reconstruct 8 or more target images, which greatly increase the information capacity of the metahologram. The crosstalk between them can be effectively reduced by carefully adjusting the feedback function in the iterative algorithm and the distance interval between the reconstruction planes. Such metahologram can be used as a platform for data storage, pattern recognition, information processing, and optical encryption. Furthermore, dielectric resonators possess low intrinsic losses, and they can support both electric and magnetic dipolar Mie-type resonances [51]. By overlapping the electric and magnetic dipolar resonances, a high transmission efficiency can be obtained [52].

On the other hand, metasurface holographic devices can overcome the limitation on polarization insensitivity of some natural materials and realize vectorial holography. For example, high-efficiency transmission-type holographic polarization multiplexing can be realized by using metasurfaces composed of anisotropic subwavelength dielectric elliptical or rectangular resonators [53]. Furthermore, combining the propagation phase and PB phase, two independent phase distributions can be imparted on any set of orthogonal polarization states (linear polarized light, circularly polarized light, or elliptically polarized light) by simultaneously modifying the sizes and orientation angles of the nanoantennas [54]. Such a method provides a new perspective for the design of polarization multiplexing metasurfaces and thus extends the application range of metasurfaces on polarization optics. On this basis, in order to make full use of all the polarization channels of the incident and output lights, a kind of all-dielectric birefringent vectorial metahologram was proposed [50]. In such a method, multiple independent phase profiles with quantified relations that can process significantly different information in different polarization channels can be realized within a single metasurface. The quantified relations of the phase distributions can be determined by analyzing the Jones matrix and polarization rotation matrix. As shown in Figure 1C, such metahologram can realize seven different polarization combinations in total 12 different polarization channels, which greatly improves the information capacity, and has many other advantages such as high fidelity, high efficiency, and wide operating bandwidth. In addition, another vectorial holography utilizing diatomic metasurfaces by varying the spatial displacement and orientation angle of the identical meta-atoms has been demonstrated [55].

In recent years, in order to improve the efficiency of polarization conversion or achieve the asymmetric transmission characteristics in specific polarization states, some multilayer cascaded metasurfaces have been proposed [56–59]. Nevertheless, these metasurfaces can only achieve asymmetric intensity transmission, reflection, or absorption, but cannot modulate the phase distribution simultaneously, which seriously limits the practical application prospects of these metasurfaces. In order to overcome this limitation, a concept for integrating holography and asymmetric light propagation is established on the basis of a two-layer cascaded metasurface [60]. In this method, a Fourier hologram is encoded into the metasurface system, which supports directional polarization encryption of holographic images. The asymmetric intensity transmission depending on propagation directions, as well as phase modulation properties of such metasurface, owes to its unique structure units the plasmonic L-shaped nanoantennas in combination with the plasmonic dimer polarizers. The phase distribution is encoded pixel-by-pixel with the combined L-dimer structure units, while the directionality of the polarization channels can be attributed to the plasmonic dimer polarizers. The designed double-layer structure is fabricated in three steps by using e-beam lithography and lift-off processes, an SiO_2 spacer is deposited between L-shaped nanoantennas and plasmonic dimer polarizers using an ion-assisted e-beam evaporator. As shown in Figure 2A, this method combines the polarization encryption hologram with the asymmetric transmission characteristics of the two-layer cascaded metasurface, so that the encoded holographic image can be observed only in particular propagation direction and polarization

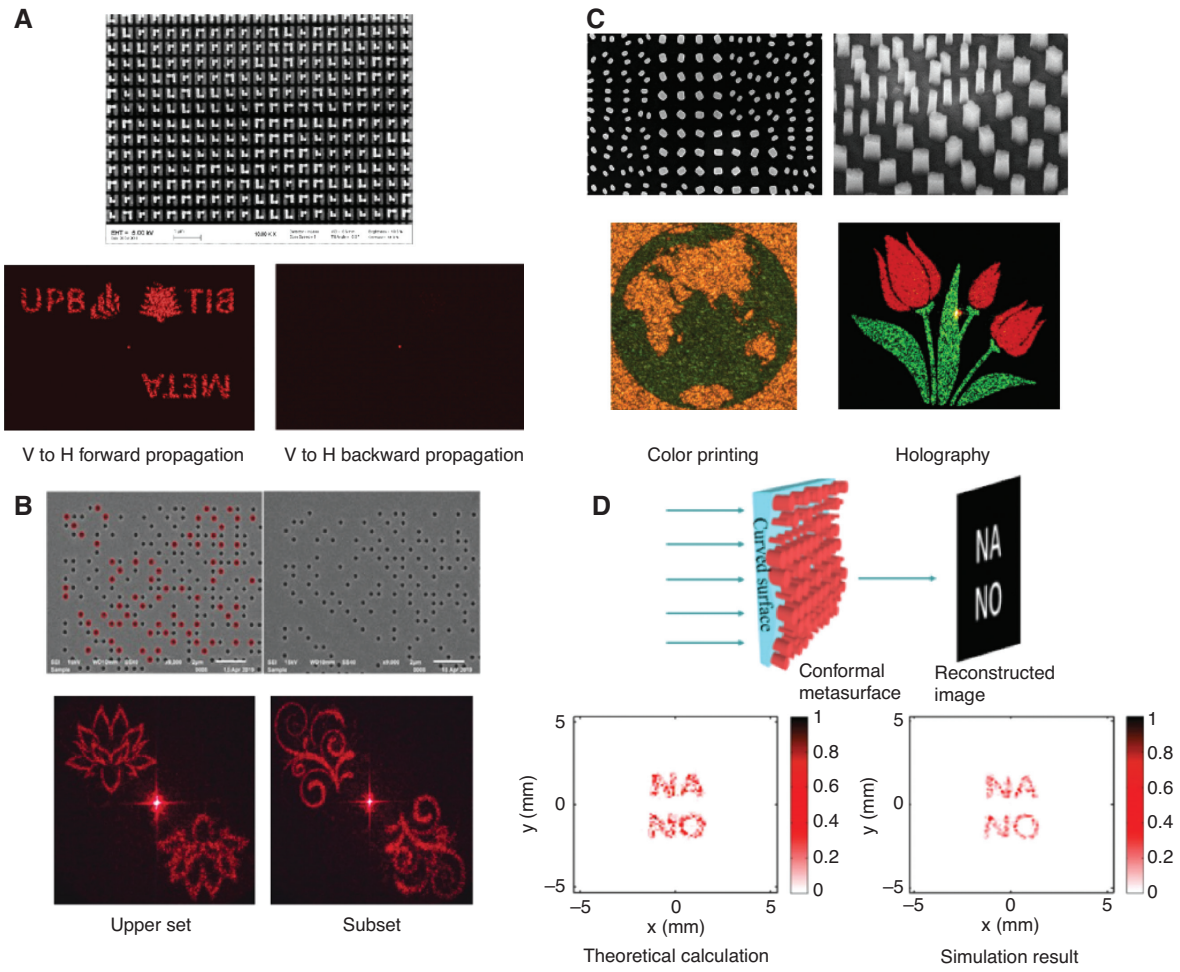

Figure 2: The integration between metasurface holography and asymmetric transmission, amplitude modulation, spectral responses and conformal metasurfaces.
(A) Scanning electron microscopy (SEM) image and experimental results of the asymmetric transmission and polarization encrypted hologram based on multilayer metasurface [60]. (B) SEM images and experimental results of two quantified relevant amplitude metaholograms based on photon sieve [61]. (C) SEM images and experimental results under dual-color printing and holography working modes of the metasurface that can modulate the spectral responses and the spatial phase information simultaneously [62]. (D) Schematic illustration, theoretical calculation result, and simulation result of a conformal metasurface wrapped on a curved surface, which is designed for curved holography (illusion) [63].

encrypted channels. Furthermore, a bilayer dielectric metasurface that can independently control two or more optical properties has been demonstrated for multiwavelength holograms and polarization-insensitive 3D holograms [64].

Usually, the metasurface wavefront modulation of the free space light depends on phase modulation. But as another design freedom, amplitude information is often neglected. This is because the amplitude modulation usually leads to lower efficiency than the phase modulation, and the quantitative control of amplitude is more difficult than a phase. Amplitude modulation usually depends on the transmission or reflection of the nanostructures, and the most common amplitude modulation method is binary amplitude modulation; that is, two values of 0 and 1 are used to encode the amplitude information. Although some works that focus on the dynamic reconfigurable phase modulation metaholograms have been proposed, the counterpart for dynamic amplitude modulation metaholograms has not been achieved so far. A quantitatively relevant amplitude hologram method based on the photon sieve was proposed and demonstrated [61]. Such a method modifies the traditional phase retrieval GS algorithm to generate binary amplitude hologram by representing the phase information in the form of amplitude. By taking the peak signal-to-noise ratio as the evaluation standard, two binary amplitude holograms with high reconstruction qualities can be obtained. And their quantified relations are established by introducing the concept of the

"holographic mask." These two binary amplitude holograms can be regarded as upper set and subset, respectively; that is, they can be transformed into each other by only writing or erasing their amplitude information. Such binary amplitude holograms with quantified relations can be encoded and processed onto two transmission-type gold film photon sieves, respectively, as shown in Figure 2B. When these two metaholograms are illuminated by visible or near-infrared incident light, two completely different reconstructed images can be reconstructed on the Fourier plane. Note that such a quantitatively correlated holographic algorithm can be further applied in dynamic metasurfaces, which can be applied in data storage, signal processing, dual-mode recognition, and other fields.

In order to reproduce complex full-color images with high fidelity, various approaches have been studied for wavelength multiplexing and multicolor metaholograms. Actually, the main challenge of realizing multicolor holography is recording and reconstructing the amplitude and phase information of different color components independently. Therefore, it is necessary to adopt an improved coding method or give each basic unit of the metasurface extra design freedom. Obviously, the most intuitive way to realize a multicolor metahologram is spatial multiplexing. Using the pixel separation method in color display technologies, multiple subcells are allocated in a single pixel to respectively arrange different nanoantennas corresponding to different wavelengths and work together to form a multicolor holographic pixel. For example, by utilizing silicon nanoblocks with different sizes as subcells and changing their in-plane orientation angles, respectively, an all-dielectric multicolor metahologram can independently modulate the phase for three wavelengths corresponding to red, green, and blue light [65]. Nevertheless, the pixel separation method is difficult to avoid the coupling between adjacent different nanoantennas. And because a multicolor pixel contains multiple subcells, its size may be no longer less than its working wavelength, which may introduce higher-order diffractions and reduce the field of view. Therefore, some works utilized broadband pixels and composite multicolor holographic coding method and successfully separated the reconstructed images of different wavelengths by using different off-axis illumination angles [66–68]. Moreover, multicolor holography can also be implemented by wavelength-decoupled metasurfaces that enable them to independently control the phase responses of each wavelength [69].

However, most of the currently reported metaholograms are designed only to encode the phase distribution or depth information, which generally appears as random or featureless pattern under incoherent illumination and cannot be used to modulate the spectral response of light. Among the existing spectral modulation applications, color printing based on metasurfaces has opened a new route of producing color images with resolution far beyond the limit of current display technologies. Significant advancements have been accomplished including the realization of color displays at the optical diffraction limit [70], polarization encoded color image [71], polarization multiplexing color printing [72–74], and also dynamic reconfigurable color printing [75]. Therefore, it is desirable to modulate simultaneously both the spatial and spectral response within a single metasurface so as to combine the metaholograms with the color printing technology, further improving the information capacity and the design freedom of metasurfaces. Some schemes have been proposed, including utilizing multilayer metasurfaces with phase plate and amplitude filters [76, 77] and utilizing the orthogonal polarization selectivity of cross antennas to achieve the *in situ* customization of color appearances and abrupt phase [78]. In addition, the reflection-type metahologram based on two kinds of dielectric parallel double-nanorod corresponding to different structural colors was also proposed [79]. Nevertheless, these methods suffer from low fabrication efficiency, relatively complex pixel design, or limited controllability. To overcome these defects, a metadevice that integrates the color printing and holographic wavelength multiplexing within a single-layer all-dielectric metasurface by modulating the spatial phase information and the spectral responses simultaneously was proposed [62]. Such a method uses amorphous silicon dimers and nanofins with optimized spectral responses to obtain the desired structural color in color printing mode. In order to encrypt multiple holographic information into a color printing pattern, a modified parallel Gerchberg–Saxton algorithm was developed to achieve the regional division of the "color-printing indexed" arrangements and obtain the different phase profiles for wavelength multiplexing independently. As shown in Figure 2C, such metasurface appears as a microscopic color image under white light illumination, while encrypting two different holographic images that can be projected at the far field when illuminated with red and green laser beams.

Apart from the planar metasurfaces, a curved object covered with a layer of ultrathin pixelated elements is called a conformal metasurface [80, 81]. Conformal metasurfaces provide extra flexibility for wavefront engineering, but they still face a series of challenges in their design and fabrication process. When the incident light passes through a curved object with an arbitrary topological profile, a random phase shift will be introduced, which results in a nonunidirectional and diffused scattering

wavefront. In consequence, the existing design theories of the conformal metasurfaces are remarkably complex; the generalized sheet transition conditions, field equivalence principle, and modified finite-difference time domain (FDTD) are used [82–84]. In order to simplify the design process of conformal metasurfaces and promote their versatility, a kind of adaptive conformal metasurface based on the Huygens principle has been proposed [63]. Utilizing the ray-tracing method or the FDTD method, the phase distribution for special functionality can be calculated according to the Maxwell equations, diffraction theory, or the holographic principle. In consideration of the optical path difference (phase difference) between the scattering surface and the target wavefront, the target transmitted phase distribution can be obtained and then arbitrarily modulated pixel-by-pixel on the conformal metasurface. Such a conformal metasurface can achieve lots of customer-designed functions under normal incidence or a small incident angle, such as focusing, anomalous refraction, cloaking, and curved holography (illusion), as shown in Figure 2D. Considering these advantages, such a conformal metasurface is suitable for integrating with any curved surface platform in practical application fields of curved screen, flexible display, wearable electronic products, medical equipment, or photoelectric devices.

3 Wavefront and polarization modulation by metasurfaces

The manipulation of different physical parameters of the wavefront is an important application of metasurfaces. The above-mentioned metaholograms mainly made use of the phase modulation ability of metasurfaces. Besides, through the reasonable principle selection and the structure design, metasurfaces can also be used for the control of other optical parameters such as amplitude, wave vector, angular momentum, and polarization state. These unique functions bring a variety of applications for metasurface, such as generation and multiplexing of vortex beams, beam shaping, complex amplitude modulation, polarization conversion, and so on.

Metasurfaces can be used for angular momentum modulation, such as generating vortex beams. Vortex beams are a kind of special beams with continuous helical phase, which can carry different values of OAM. They have a unique "doughnut-shaped" energy distribution. The phase distribution can be expressed as $\exp(il\varphi)$, where l is the topological charge of the vortex beam. Taking the advantage of unique orthogonal characteristics between different OAM modes, the devices based on vortex beams have received increasing attention for its various applications such as optical storage of large-capacity data, information coding, quantum key distribution, laser processing, manipulation of biological cells, and so on [85, 86].

Traditional approaches for generating optical vortices include helical phase plates, CGHs, and the conversion of Hermite–Gaussian mode to Laguerre–Gaussian mode. In comparison, owing to the ultrathin and broadband characteristics, some methods of generating vortex beams by metasurfaces were proposed [87]. However, the reported methods are usually only applicable to generate a single or a finite number of optical vortices with a specific topological charge. In practical applications, it is often necessary to generate a large number of vortex beam arrays with different topological charges in a finite space. A volumetric optical vortices generation method based on dielectric metasurfaces was proposed [88]. Such metasurface encodes the phase distribution of the Dammann vortex grating (DVG) with optimization and employs the spiral Dammann zone plate (SDZP) together with a lens factor to expand the optical vortex array into 3D. The DVG is an improved design that integrates the blazing grating with a spiral phase pattern to create a two-dimensional vortex array in the x-y plane with uniform energy distribution. And the SDZP is essentially a Dammann zone plate integrated into a spiral phase profile to redistribute the energy uniformly into several longitudinal coaxial vortices. Specifically, the topological charge of each vortex is determined by its corresponding diffraction orders in x, y, z directions. The topological charges can be actively controlled by adjusting the angular momentum of the incident light. In addition, by introducing this new freedom of OAM, a variety of new optical communication systems that use OAM to increase their information capacity can be successfully designed. Currently, one of the main challenges of the fiber communication system based on vortex beams lies in multiplexing OAM via a kind of effective, compact, and flexible method. Hence, an approach based on a predesigned reflective metasurface was proposed to achieve the generation of collinear vortex beams with different OAMs by different incident angles [89]. Compared with the traditional OAM generation methods, this approach shows superiorities of broadband operating wavelength, high mode purity, and compact size. A free space OAM multiplexing communication experiment based on a single metasurface was carried out by utilizing such a method. Using two different polarization states and four kinds of vortex beams with different topological charges, 448 Gbit/s data transmission by 28-GBaud QPSK signals can be performed.

Bessel beams exhibit nondiffractive, self-healing characteristics and thus have various applications in optical alignment, interconnection, molecular detection, microscopic imaging, and other areas [90, 91]. Traditionally, Bessel beams are generated using axicons, diffractive optical elements, or spatial light modulators. Nevertheless, these methods are usually limited by the large device volume, low transmission efficiency, limited numerical aperture, and other issues. For breaking these limits, a method of generating a Bessel beam array based on a dielectric Huygens' metasurface was proposed [92]. This method integrates the phase profiles of Dammann grating and the axicon into a single metasurface and optimizes its phase distribution to realize the beam splitting with uniform intensity. Such Huygens' metasurface can effectively produce a high-efficiency Bessel beam array with long propagation distance.

For some complex optical field distributions, such as perfect holographic imaging and reconstructing the characteristics of diffuse scattering surface, the phase or amplitude-only modulation of a single degree of freedom often cannot meet the practical requirements. Therefore, to achieve full complex amplitude control, a metasurface that enables to modulate both the amplitude and phase simultaneously and independently is desired. In previous works, the nanoantennas used for complex amplitude modulation include the C-shaped nanoantennas [93], X-shaped nanoantennas [94], and so on. However, most of these works either are limited to the terahertz and microwave band or require relatively complex pixel design and high processing accuracy, which limit the modulation range of the complex amplitude modulation. Therefore, a method of realizing full complex amplitude modulation by using an ultrathin dielectric metasurface that consists of silicon nanofins with different cross-sections has been proposed [95]. This method can be used for generating a uniform or tailored intensity distribution in a number of one- or two-dimensional diffraction orders to achieve the selective excitation. In such dielectric metasurface, the final result of the wavefront modulation is indeed the integration of the PB phase, which comes from the orientation angles of the nanofins and the dynamic phase generated from the different geometric parameters of the nanofins. As shown in Figure 3A, in order to verify the above method, the selected diffraction orders of the sample constitute a pattern of "META," while all other unselected diffraction orders are suppressed. Using similar methods, independent and complete control of amplitude and phase at up to two optical frequencies based on all-dielectric metasurfaces was demonstrated [98]. Except for the free space

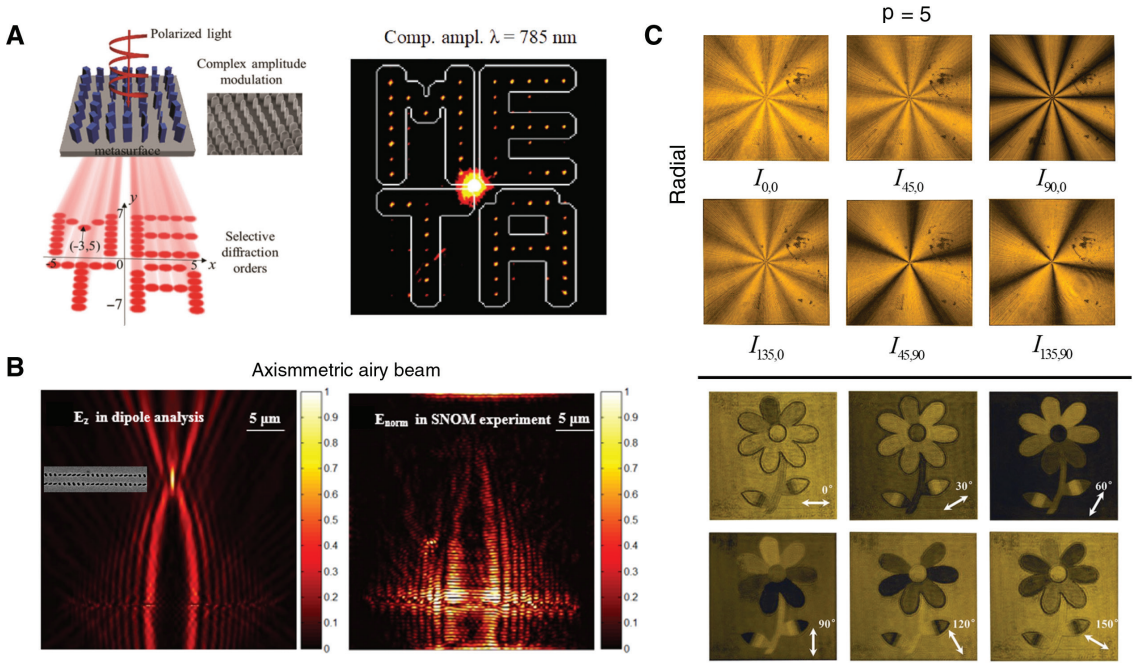

Figure 3: Wavefront and polarization modulation by metasurfaces.
(A) Schematic illustration and experimental results of the complex amplitude modulation for arbitrary two-dimensional diffraction order distribution with a dielectric metasurface [95]. (B) Near-field plasmonic beam engineering with complex amplitude modulation based on metasurface [96]. (C) The measured intensity distributions of the high-order radial polarization beams generated by the metasurface composed by silicon nanofins and the polarization encryption images based on such metasurface [97].

propagating light field, the above complex amplitude modulation method can also be used to tailor the surface plasmon polaritons (SPPs). For example, a method of effectively manipulating the complex amplitude of SPPs with arbitrary complex fields in the near-field regime based on metasurfaces composed of nanoaperture arrays was demonstrated [96]. By changing the orientation angles of individual nanoapertures and simultaneously tuning their geometric parameters, the phase and amplitude can be controlled independently. Such a method can be used to generate Airy plasmons and axisymmetric Airy SPPs. As shown in Figure 3B, the SPP's trajectory and the location of the hotspot in the experimental result are consistent with the design. This metasurface complex amplitude modulation method for SPPs has potential application value in many fields, such as plasma beam shaping, integrated optoelectronic system, surface wave holography, and so on.

To fully characterize the characteristics of the electromagnetic wave, not only the magnitude of the complex amplitude of the field, but also the polarization direction should be considered. The polarization manipulation can be realized by splitting the incident light into two orthogonal components and controlling the required phase delay between them. Conventional methods for the polarization manipulation are mainly based on natural birefringent materials, such as anisotropic crystal and liquid crystals, which exhibit anisotropic property along the ordinary and extraordinary axes. However, the traditional methods face many disadvantages including narrow bandwidth, bulky size, and limited choice of materials, while metasurfaces can induce strong birefringence by properly designed anisotropic nanoantennas and promise a broad prospect in polarization optics. Through the precise design of single-layer or multilayer metasurfaces, a variety of polarization control schemes have been proposed [99, 100]. For example, a metasurface consists of deliberately designed achiral twofold mirror symmetry Ω-shaped nanoantennas that were proposed [101]. By taking advantage of the birefringence effect and reflection-type MIM hierarchy, such metasurface provides high conversion efficiency and a wide working band in the near-infrared band. Note that the majority of the reported strategies for polarization modulation based on metasurfaces were designed only for spatially homogeneous polarized beams, while less attention has been devoted to spatially variant inhomogeneous vector beams and polarization encryption schemes. Cylindrical vector (CV) beams are a typical group of vector beams that are solutions of the vector wave equation and possess spatially inhomogeneous states of polarization, which obey cylindrical symmetry with respect to their propagation directions. Again, metasurfaces can conquer the traditional complex experimental setups and bulky devices, realizing a more compact device [97]. As shown in Figure 3C, with the same geometric size and different local orientation angles, nanofins can work as subwavelength half-wave plates to manipulate the polarization direction of the output light field and generate arbitrary high-order CV beams. In addition, the polarization states' spatial distribution of the CV beams can be switched by varying the polarization states of the incident light. Furthermore, using the same principle, an image can be encrypted onto a metasurface that possesses spatial inhomogeneous polarization states for anticounterfeiting applications.

4 Dynamically tunable metasurfaces

Due to the limitation of processing ability, material characteristics, and fixed structures, although metasurfaces have excellent electromagnetic manipulation ability, it is still a remarkably challenging task to design a reconfigurable metasurface that works in the near-infrared and visible light band. A method that uses a mechanically stretchable substrate to realize the dynamic switching of the reconstructed image at a specific distance was demonstrated [102]. Another noteworthy way is to adjust the resonance properties of the nanoantennas by introducing materials with tunable physical properties such as phase change materials and two-dimensional materials. Phase change materials, such as germanium antimony telluride (GST), indium antimonide, gallium lanthanum sulfide, and vanadium oxide (VO_2), are commonly used to construct dynamically tunable metasurfaces. Under appropriate thermal, optical, or electrical stimulation, their atomic arrangements can be switched between amorphous and crystalline (or semiconducting and metallic) states, is which called the "phase transition process." The physical properties of phase change materials remain stable at room temperature and come with gradual change after the phase transition process. This transition is reversible and nonvolatile and can be flexibly controlled at high speed. Because of these unique properties, phase change materials show great potential in designing dynamically tunable metasurfaces.

Many novel multifunctional compact devices have been designed through the integration of phase-change materials and metasurfaces, such as tunable metalens with variable focuses, tunable wave plate based on resonance V-shaped antennas, polarization converter, color/multi-wavelength selective diffractive devices, and mimicking

synapse [103–107]. Among these applications, the metasurface consists of V-shaped plasmonic antennas, and an interval modulation layer made of the phase change material GST for active phase control is a typical example [108]. As shown in Figure 4A, periodically arranged GST strips and silicon strips between the V-shaped plasmonic antennas and substrate were utilized as an interval modulation layer. Because the resonance of plasmonic structures is very sensitive to the surrounding dielectric environment, one can effectively change the scattering phases of the V-shaped plasmonic antennas through actively controlling the optical property of GST. By controlling the phase delay between the scattering waves from the two subunits, the phase difference between the two coherent orthogonally polarized beams can be modulated, and a flexible and high-speed dynamic tunable polarization converter for the mid-infrared band is realized. On the other hand, GST can also be used in the fields of beam deflection and dynamic holographic display. Using two kinds of U-shaped GST nanoantennas exhibiting remarkably different resonance behaviors at the crystal and amorphous states, an active wavefront switching metasurface at near-infrared spectral bands was demonstrated [110].

It is worth noting that although the phase change materials could offer tunable optical properties, their operating wavelength range and phase transition conditions are different from each other. Notably, VO_2 has a lower phase transition threshold over other phase change materials, and its operating band can reach near-infrared or even visible range. As an example, hybrid reconfigurable metasurface for dynamic control of mode modulation and spatial multiplexing was proposed [111]. Such metasurface is composed of composite concentric rings (CCRs) with different ratios of gold and VO_2. By considering the optical properties of VO_2, the CCRs can operate as concentric rings under a metallic state with relatively high conductivity, while functioning as split rings under semiconductor state. Therefore, by delicately designing the geometric parameters, such metasurface can generate vortex beams or diffraction lobes respectively through fulfilling the requirement of amplitude and phase at both states.

In addition, dynamic tunable devices based on magnesium (Mg) provide another potential solution for reconfigurable optical elements. As an active material, Mg exhibits excellent metallic properties at optical frequency, but when Mg is hydrogenated to Mg hydride (MgH_2), its optical properties will change remarkably. This transition is reversible through dehydrogenation by oxygen. As a result, the plasmonic response of Mg nanoantennas can be reversibly switched on and off, constituting subwavelength dynamic plasmonic pixels. On this basis, by

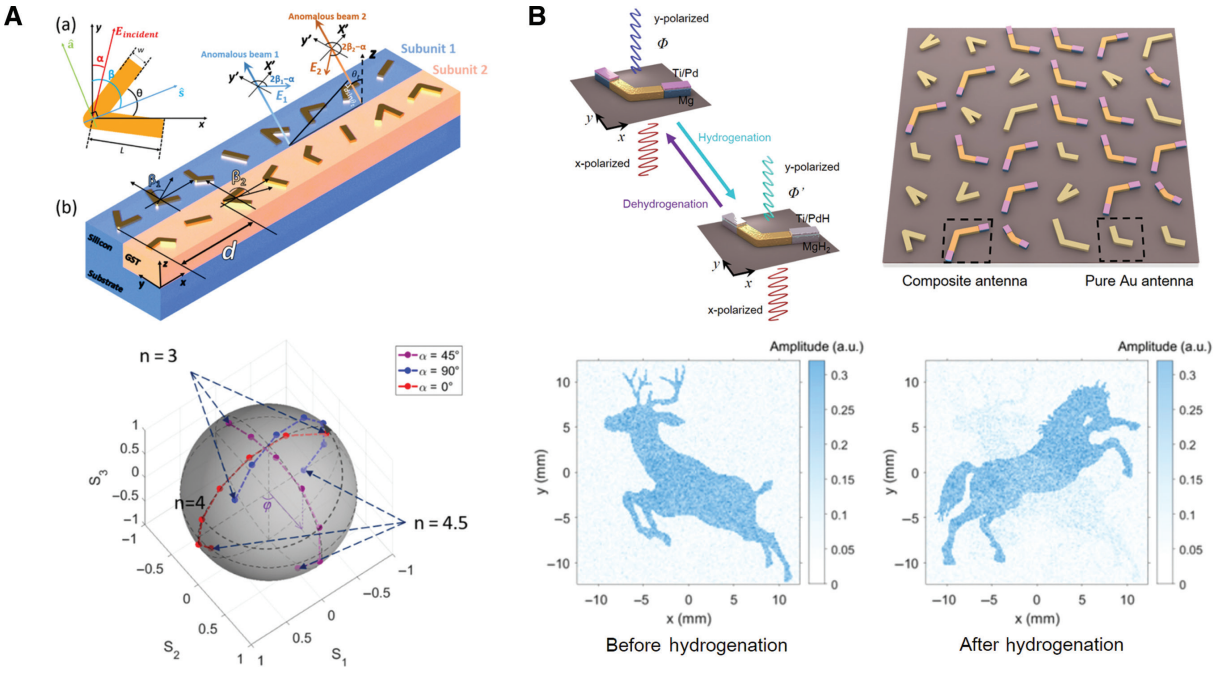

Figure 4: Dynamically tunable metasurfaces.
(A) Schematic of the metasurface for active tunability of the ellipticity of anomalously diffracted beams [108]. (B) Schematic diagram and simulation results of the addressable dynamic metasurface holographic display method based on pure gold V-shaped antennas and composite gold/Mg V-shaped antennas [109].

using spatial interlaced gold nanorods and Mg nanorods as independent subunits, a PB phase metasurface can be formed with two independent phase profiles determined by Mg and Au nanorods as dynamic and static pixels, respectively [112]. By doing so, dynamic metaholograms for advanced optical information processing and encryption can be achieved. However, due to its multiple subunits, this method belongs to spatial multiplexing, which inevitably reduces the available spatial bandwidth product of the holograms. In order to overcome this defect, a switchable metasurface phase-only hologram based on the hydrogenation/dehydrogenation process of composite gold–Mg nanoantennas was proposed [109]. Such metasurface consists of pure gold V-shaped antennas with fixed scattering phase as the static pixels and composite Mg–gold V-shaped antennas with a switchable scattering phase as the dynamic pixels. An iterative algorithm was proposed to realize the phase retrieval of two phase-only holograms with a predesigned quantified relationship. As shown in Figure 4B, by utilizing hierarchical reaction kinetics of Mg upon the hydrogenation and dehydrogenation process, a dynamic metahologram that can switch two totally different target images theoretically was proposed. Further efforts on dynamic metasurfaces are still in progress, including dynamic color display [113], rewritable metacanvas [114], reprogrammable metasurfaces with diodes [115], and so on.

5 Nonlinear metasurfaces

In theoretical framework, the nonlinear phenomenon resulted from the nonlinear polarization, which can be expressed as follows:

$$\mathbf{P} = \varepsilon_0 \boldsymbol{\chi}^{(1)} \cdot \mathbf{E} + \varepsilon_0 \boldsymbol{\chi}^{(2)} : \mathbf{EE} + \varepsilon_0 \boldsymbol{\chi}^{(3)} \vdots \mathbf{EEE} + \cdots = \mathbf{P}_{\mathrm{L}} + \mathbf{P}_{\mathrm{NL}} \qquad (2)$$

where ε_0 is the dielectric constant in vacuum, and $\mathbf{E}$ is the complex amplitude of the fundamental incident light. $\boldsymbol{\chi}^{(1)}$ represents the linear susceptibility, and $\boldsymbol{\chi}^{(2)}$ and $\boldsymbol{\chi}^{(3)}$ indicate the second- and third-order characteristic nonlinear susceptibility tensors, respectively. In general, the high-order nonlinear susceptibility tensors are relatively small; hence, high field enhancement is required for generating the nonlinear frequency components.

Achieving the nonlinear modulation of an electromagnetic wave by using metasurfaces has become a hot topic. Because metasurfaces can relax the phase-matching conditions for harmonic generation and can provide extra confinement and large field enhancement for high-efficiency nonlinear effect, in this context nonlinear metasurfaces come into the field of vision. Such metasurfaces utilize the nonlinear effect produced by the interaction between the intense light field (such as femtosecond laser pulse) and their nanoantennas to generate a nonlinear effect. Meanwhile, through spatial modulation, the wavefront of newly generated frequencies can be modulated, which surpasses all the former research aspects of nonlinear optics and provides extra multiplexing channels. By elaborately designing the nanoantennas of the nonlinear metasurfaces and properly optimizing the phase retrieval algorithms of the holograms, two or more completely different target images can be reconstructed at the linear frequency and the nonlinear frequency, simultaneously. For example, the spin and wavelength multiplexing nonlinear metasurface holography, which uses nonlinear PB phase modulation mechanism, can realize the independent reconstruction of multiple different target images at the fundamental frequency and the second harmonic frequency with spin dependence [116]. Meanwhile, the double-layer nonlinear metasurface composed of V-shaped nanoantennas can realize the polarization multiplexing of the second harmonic wave [117].

The nonlinear frequency conversion and wavefront modulation based on plasmonic metasurfaces have been demonstrated by many reported works. However, the application of plasmonic metasurfaces in nonlinear nanophotonics is severely limited by many factors including large loss and low optical damage threshold. On the contrary, high refractive index all-dielectric metasurfaces have proved to be promising candidates for nonlinear applications because they can overcome the aforementioned limitations. Due to their relatively large values of refractive indexes and low loss, all-dielectric metasurfaces have larger damage threshold compared to their plasmonic counterparts, which enables operation with large pump intensities and supports stronger nonlinear optical responses. These advantages make all-dielectric metasurfaces a powerful platform for nonlinear nanophotonics. A method of nonlinear full wavefront modulation for the third harmonic generation with silicon metasurfaces was proposed [118]. Such a method uses the nonlinear PB phase modulation mechanism to encode the phase gradient on the silicon metasurface, and the polarization dependence of anomalous refraction is demonstrated experimentally. Furthermore, as shown in Figure 5A, the nonlinear PB phase offers different phase modulation factors for different polarization states of the third harmonic wave, which are helpful for realizing holographic multiplexing and high-fidelity reconstruction. This method remarkably eases the design and fabrication processes of nonlinear metasurfaces and paves the way to an

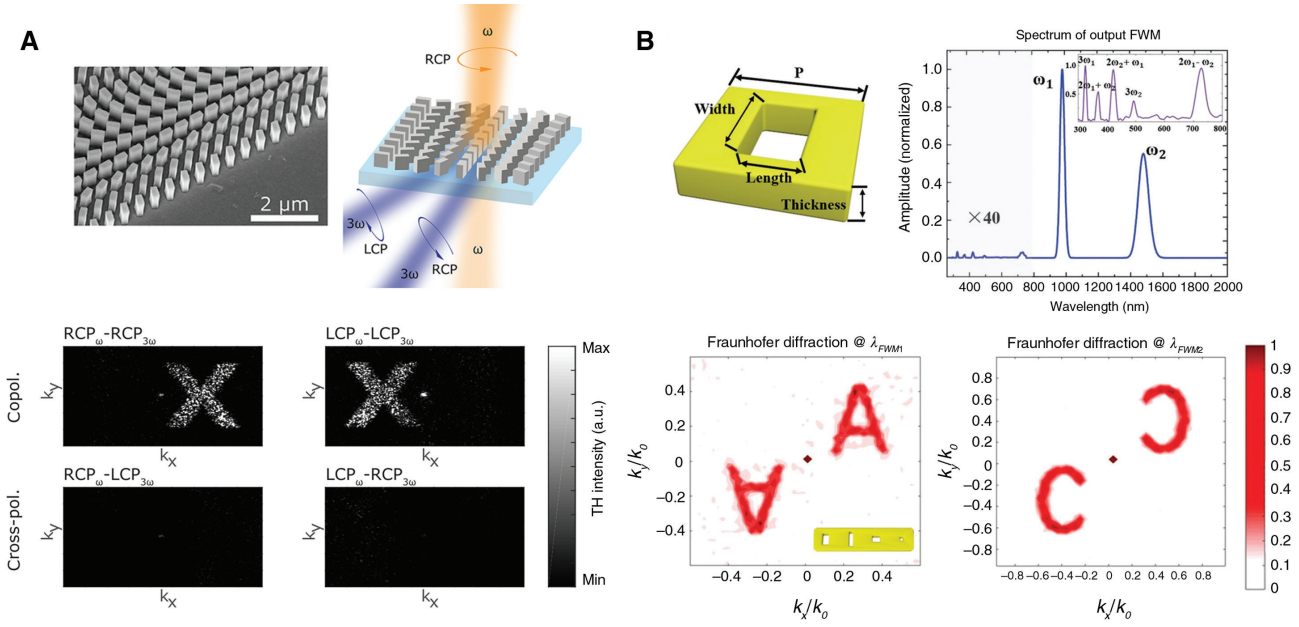

Figure 5: Nonlinear metasurfaces.
(A) Scanning electron microscopy image of the geometric phase nonlinear silicon metasurface and its measured holographic reconstructed images for different combinations of the input and output polarizations [118]. (B) Schematic illustration and simulation results of the four-wave mixing nonlinear holography based on a gold nanoaperture metasurface [119].

easy-to-use toolbox for nonlinear wavefront modulation with all-dielectric metasurfaces.

While the previous works mainly focus on the harmonic generation, the more general wavefront tailoring for four-wave mixing (FWM) process has not been fully explored. The nonlinear frequency signal generated by the FWM effect can cover multiple wavelengths, which has great application potential for expanding information capacity. An FWM holographic multiplexing method based on nonlinear metasurfaces composed of aperture arrays on freestanding gold film was proposed [119]. By tailoring the geometric sizes of these apertures, the complex amplitude modulation of the nonlinear frequency components for FWM can be achieved. Two binary amplitude-only holograms have been achieved at different FWM wavelengths through one single metasurface. As shown in Figure 5B, when two incident femtosecond pulses with different carrier frequencies illuminate such metasurface, the spatial multiplexing and frequency multiplexing for nonlinear holography can be achieved simultaneously.

The above results show that nonlinear metasurfaces have wide application prospects in arbitrary frequency conversion, holographic multiplexing, optical encryption, and anticounterfeiting. In addition, they can also be used in nonlinear color holographic display, transform optics, data storage, and other related fields.

6 Summary

In summary, metasurfaces have surpassed the limitations of traditional optical and bulky metamaterials, showing unprecedented wavefront modulation ability. Its inherent ultrathin and compact properties, as well as the pixel-by-pixel subwavelength spatial light field manipulation ability, provide a new approach for the miniaturization and integration of optical devices. Here we briefly review the recent progress of metasurfaces in the field of holographic display, wavefront modulation and polarization conversion, dynamically tunable metasurfaces, and nonlinear wavefront manipulation. It should be noted that these fields are far from all; many excellent works have been proposed and demonstrated. Moreover, as new types of materials in this field, lead halide perovskites, graphene, and topological insulator materials have also been introduced into the design of metasurfaces in recent years, which are used for nonlinear harmonic generation [120], variable and reversible color printing [121], and metasurface holography [122, 123]. Different material properties will bring different functions and characteristics. Therefore, the updating and expansion of materials will be an important field for further exploration. Thanks to the design flexibility, tunability, and multifunctionality, metasurfaces can be widely used in a variety of applications. However, the novel design fields of metasurfaces,

such as cascaded metasurfaces, dynamically reconfigurable metasurfaces and nonlinear metasurfaces still need to be further investigated. Many theoretical and experimental challenges need to be solved, such as coupling and alignment accuracy between cascaded metasurfaces, the large modulation depth of the dynamically tunable metasurfaces, and even real-time pixel-by-pixel modulation abilities. Meanwhile, the practical engineering applications of metasurfaces are still facing lot of limits, such as fabrication difficulties and high cost. The combination with practical engineering applications will also be one of the major efforts for researchers in the future.

Funding: The authors acknowledge the funding provided by Beijing Outstanding Young Scientist Program (BJJWZYJH01201910007022), National Natural Science Foundation of China (no. 61775019) program, NSFC-DFG joint program (NSFC no. 61861136010, DFG no. ZE953/11-1), Beijing Municipal Natural Science Foundation (no. 4172057, Funder Id: http://dx.doi.org/10.13039/501100004826), Beijing Nova Program (no. Z171100001117047, Funder Id: http://dx.doi.org/10.13039/501100005090), and Fok Ying-Tong Education Foundation of China (no. 161009). T.Z. acknowledged the support from the European Research Council under the European Union's Horizon 2020 research and innovation program (grant agreement no. 724306).

References

[1] Zhang L, Mei S, Huang K, Qiu C. Advances in full control of electromagnetic waves with metasurfaces. Adv Opt Mater 2016;4:818–33.
[2] Hsiao H, Cheng H, Tsai D. Fundamentals and applications of metasurfaces. Small Methods 2017;1:1600064.
[3] Ding F, Pors A, Bozhevolnyi SI. Gradient metasurfaces: a review of fundamentals and applications. Rep Prog Phys 2018;81:26401.
[4] Chen S, Li Z, Zhang Y, Cheng H, Tian J. Phase manipulation of electromagnetic waves with metasurfaces and its applications in nanophotonics. Adv Opt Mater 2018;6:1800104.
[5] Sung J, Lee G, Lee B. Progresses in the practical metasurface for holography and lens. Nanophotonics 2019;8:1701–18.
[6] Genevet P, Capasso F, Aieta F, Khorasaninejad M, Devlin R. Recent advances in planar optics: from plasmonic to dielectric metasurfaces. Optica 2017;4:139–52.
[7] Genevet P, Capasso F. Holographic optical metasurfaces: a review of current progress. Rep Prog Phys 2015;78:24401.
[8] Wan W, Gao J, Yang X. Metasurface holograms for holographic imaging. Adv Opt Mater 2017;5:1700541.
[9] Huang L, Zhang S, Zentgraf T. Metasurface holography: from fundamentals to applications. Nanophotonics Berlin 2018;7:1169–90.
[10] Yang Y, Wang W, Moitra P, et al. Dielectric meta-reflectarray for broadband linear polarization conversion and optical vortex generation. Nano Lett 2014;14:1394–9.
[11] Huang K, Liu H, Restuccia S, et al. Spiniform phase-encoded metagratings entangling arbitrary rational-order orbital angular momentum. Light Sci Appl 2018;7:17156.
[12] Chen Y, Yang X, Gao J. Spin-selective second-harmonic vortex beam generation with Babinet-inverted plasmonic metasurfaces. Adv Opt Mater 2018;6:1800646.
[13] Pegard NC, Fleischer JW. Optimizing holographic data storage using a fractional Fourier transform. Opt Lett 2011;36:2551–3.
[14] Goh XM, Zheng Y, Tan SJ, et al. Three-dimensional plasmonic stereoscopic prints in full colour. Nat Commun 2014;5:5361.
[15] Jin L, Dong Z, Mei S, et al. Noninterleaved metasurface for (2^6–1) spin- and wavelength-encoded holograms. Nano Lett 2018;18:8016–24.
[16] Liu H, Yang B, Guo Q, et al. Single-pixel computational ghost imaging with helicity-dependent metasurface hologram. Sci Adv 2017;3:e1701477.
[17] Chen WT, Zhu AY, Sanjeev V, et al. A broadband achromatic metalens for focusing and imaging in the visible. Nat Nanotechnol 2018;13:220.
[18] Wang S, Wu PC, Su V, et al. A broadband achromatic metalens in the visible. Nat Nanotechnol 2018;13:227–32.
[19] Wang S, Wu PC, Su V, et al. Broadband achromatic optical metasurface devices. Nat Commun 2017;8:187.
[20] Ma Z, Li Y, Li Y, et al. All-dielectric planar chiral metasurface with gradient geometric phase. Opt Express 2018;26:6067–78.
[21] Pan C, Ren M, Li Q, Fan S, Xu J. Broadband asymmetric transmission of optical waves from spiral plasmonic metamaterials. Appl Phys Lett 2014;104:121112.
[22] Bao Y, Yu Y, Xu H, et al. Coherent pixel design of metasurfaces for multidimensional optical control of multiple printing-image switching and encoding. Adv Funct Mater 2018;28:1805306.
[23] Minovich AE, Miroshnichenko AE, Bykov AY, et al. Functional and nonlinear optical metasurfaces. Laser Photonics Rev 2015;9:195–213.
[24] Xiao Y, Qian H, Liu Z. Nonlinear metasurface based on giant optical Kerr response of gold quantum wells. ACS Photonics 2018;5:1654–9.
[25] Li G, Wu L, Li KF, et al. Nonlinear metasurface for simultaneous control of spin and orbital angular momentum in second harmonic generation. Nano Lett 2017;17:7974–9.
[26] Minerbi E, Keren-Zur S, Ellenbogen T. Nonlinear metasurface fresnel zone plates for terahertz generation and manipulation. Nano Lett 2019;19:6072–7.
[27] Li G, Zhang S, Zentgraf T. Nonlinear photonic metasurfaces. Nat Rev Mater 2017;2:17010.
[28] Yu N, Genevet P, Kats MA, et al. Light propagation with phase discontinuities: generalized laws of reflection and refraction. Science 2011;334:333–7.
[29] Kats MA, Genevet P, Aoust G, et al. Giant birefringence in optical antenna arrays with widely tailorable optical anisotropy. P Natl Acad Sci USA 2012;109:12364–8.
[30] Pfeiffer C, Emani NK, Shaltout AM, et al. Efficient light bending with isotropic metamaterial Huygens' surfaces. Nano Lett 2014;14:2491–7.
[31] Wang L, Kruk S, Tang H, et al. Grayscale transparent metasurface holograms. Optica 2016;3:1504–5.

[32] Decker M, Staude I, Falkner M, et al. High-efficiency dielectric Huygens' surfaces. Adv Opt Mater 2015;3:813–20.
[33] Schnars U, Falldorf C, Watson J, Jüptner W. Digital holography and wavefront sensing: principles, techniques and applications. Berlin, Germany: Springer Verlag, 2015.
[34] Poon TC, Liu JP. Introduction to modern digital holography: with matlab. New York: Cambridge University Press, 2014.
[35] Huang L, Chen X, Muehlenbernd H, et al. Three-dimensional optical holography using a plasmonic metasurface. Nat Commun 2013;4:2808.
[36] Wei Q, Huang L, Li X, Liu J, Wang Y. Broadband multiplane holography based on plasmonic metasurface. Adv Opt Mater 2017;5:1700434.
[37] Zheng G, Muehlenbernd H, Kenney M, et al. Metasurface holograms reaching 80% efficiency. Nat Nanotechnol 2015;10:308–12.
[38] Sung J, Lee G, Choi C, Hong J, Lee B. Single-layer bifacial metasurface: full-space visible light control. Adv Opt Mater 2019;7:1801748.
[39] Huang K, Liu H, Garcia-Vidal FJ, et al. Ultrahigh-capacity non-periodic photon sieves operating in visible light. Nat Commun 2015;6:7059.
[40] Chen Y, Yang X, Gao J. Spin-controlled wavefront shaping with plasmonic chiral geometric metasurfaces. Light Sci Appl 2018;7:1–10.
[41] Franklin D, Modak S, Vazquez-Guardado A, Safaei A, Chanda D. Covert infrared image encoding through imprinted plasmonic cavities. Light Sci Appl 2018;7:93.
[42] Shi Z, Khorasaninejad M, Huang Y, et al. Single-layer metasurface with controllable multiwavelength functions. Nano Lett 2018;18:2420–7.
[43] Kamali SM, Arbabi E, Arbabi A, et al. Angle-multiplexed metasurfaces: encoding independent wavefronts in a single metasurface under different illumination angles. Phys Rev X 2017;7:41056.
[44] Wang Q, Zhang X, Plum E, et al. Polarization and frequency multiplexed terahertz meta-holography. Adv Opt Mater 2017;5:1700277.
[45] Deng J, Yang Y, Tao J, et al. Spatial frequency multiplexed meta-holography and meta-nanoprinting. ACS Nano 2019;13:9237–46.
[46] Ren H, Briere G, Fang X, et al. Metasurface orbital angular momentum holography. Nat Commun 2019;10:1–8.
[47] Montelongo Y, Tenorio-Pearl JO, Williams C, et al. Plasmonic nanoparticle scattering for color holograms. P Natl Acad Sci Usa 2014;111:12679–83.
[48] Wen D, Yue F, Li G, et al. Helicity multiplexed broadband metasurface holograms. Nat Commun 2015;6:8241.
[49] Huang L, Muhlenbernd H, Li X, et al. Broadband hybrid holographic multiplexing with geometric metasurfaces. Adv Mater 2015;27:6444.
[50] Zhao R, Sain B, Wei Q, et al. Multichannel vectorial holographic display and encryption. Light Sci Appl 2018;7:95.
[51] Ginn JC, Brener I, Peters DW, et al. Realizing optical magnetism from dielectric metamaterials. Phys Rev Lett 2012;108:974029.
[52] Shalaev MI, Sun J, Tsukernik A, et al. High-efficiency all-dielectric metasurfaces for ultracompact beam manipulation in transmission mode. Nano Lett 2015;15:6261–6.
[53] Arbabi A, Horie Y, Bagheri M, Faraon A. Dielectric metasurfaces for complete control of phase and polarization with subwavelength spatial resolution and high transmission. Nat Nanotechnol 2015;10:190–937.
[54] Mueller JPB, Rubin NA, Devlin RC, Groever B, Capasso F. Metasurface polarization optics: independent phase control of arbitrary orthogonal states of polarization. Phys Rev Lett 2017;118:113901.
[55] Deng Z, Deng J, Zhuang X, et al. Diatomic metasurface for vectorial holography. Nano Lett 2018;18:2885–92.
[56] Liu D, Xiao Z, Ma X, Wang Z. Asymmetric transmission of linearly and circularly polarized waves in metamaterial due to symmetry-breaking. Appl Phys Express 2015;8:52001.
[57] Menzel C, Helgert C, Rockstuhl C, et al. Asymmetric transmission of linearly polarized light at optical metamaterials. Phys Rev Lett 2010;104:253902.
[58] Ji R, Wang S, Liu X, Lu W. Giant and broadband circular asymmetric transmission based on two cascading polarization conversion cavities. Nanoscale 2016;8:8189–94.
[59] Pfeiffer C, Zhang C, Ray V, Guo LJ, Grbic A. High performance bianisotropic metasurfaces: asymmetric transmission of light. Phys Rev Lett 2014;113:23902.
[60] Frese D, Wei Q, Wang Y, Huang L, Zentgraf T. Nonreciprocal asymmetric polarization encryption by layered plasmonic metasurfaces. Nano Lett 2019;19:3976–80.
[61] Xu Z, Huang L, Li X, et al. Quantitatively correlated amplitude holography based on photon sieves. Adv Opt Mater 2019:1901169.
[62] Wei Q, Sain B, Wang Y, et al. Simultaneous spectral and spatial modulation for color printing and holography using all-dielectric metasurfaces. Nano Lett 2019:9b03957.
[63] Han N, Huang L, Wang Y. Illusion and cloaking using dielectric conformal metasurfaces. Opt Express 2018;26:31625–35.
[64] Zhou Y, Kravchenko II, Wang H, et al. Multifunctional metaoptics based on bilayer metasurfaces. Light Sci Appl 2019;8:1–9.
[65] Wang B, Dong F, Li Q, et al. Visible-frequency dielectric metasurfaces for multiwavelength achromatic and highly dispersive holograms. Nano Lett 2016;16:5235–40.
[66] Zhang X, Pu M, Guo Y, et al. Colorful metahologram with independently controlled images in transmission and reflection spaces. Adv Funct Mater 2019;29:1809145.
[67] Wan W, Gao J, Yang X. Full-Color plasmonic metasurface holograms. ACS Nano 2016;10:10671–80.
[68] Li X, Chen L, Li Y, et al. Multicolor 3D meta-holography by broadband plasmonic modulation. Sci Adv 2016;2:e1601102.
[69] Yoon G, Kim J, Mun J, et al. Wavelength-decoupled geometric metasurfaces by arbitrary dispersion control. Commun Phys 2019;2:1–7.
[70] Kumar K, Duan H, Hegde RS, et al. Printing colour at the optical diffraction limit. Nat Nanotechnol 2012;7:557–61.
[71] Zang X, Dong F, Yue F, et al. Polarization encoded color image embedded in a dielectric metasurface. Adv Mater 2018;30:1707499.
[72] Nagasaki Y, Suzuki M, Takahara J. All-dielectric dual-color pixel with subwavelength resolution. Nano Lett 2017;17:7500–6.
[73] Li Z, Clark AW, Cooper JM. Dual color plasmonic pixels create a polarization controlled nano color palette. ACS Nano 2016;10:492–8.
[74] Yang B, Liu W, Li Z, et al. Polarization-sensitive structural colors with hue-and-saturation tuning based on all-dielectric nanopixels. Adv Opt Mater 2018;6:1701009.
[75] Duan X, Kamin S, Liu N. Dynamic plasmonic colour display. Nat Commun 2017;8:14606.

[76] Hu Y, Luo X, Chen Y, et al. 3D-integrated metasurfaces for full-colour holography. Light Sci Appl 2019;8:1–9.
[77] Lim KTP, Liu H, Liu Y, Yang JKW. Holographic colour prints for enhanced optical security by combined phase and amplitude control. Nat Commun 2019;10:25.
[78] Zhang Y, Shi L, Hu D, et al. Full-visible multifunctional aluminium metasurfaces by in situ anisotropic thermoplasmonic laser printing. Nanoscale Horiz 2019;4:601–9.
[79] Yoon G, Lee D, Nam KT, Rho J. "Crypto-display" in dual-mode metasurfaces by simultaneous control of phase and spectral responses. ACS Nano 2018;12:6421–8.
[80] Khorasaninejad M, Chen WT, Devlin RC, et al. Metalenses at visible wavelengths: diffraction-limited focusing and subwavelength resolution imaging. Science 2016;352:1190–4.
[81] Kamali SM, Arbabi A, Arbabi E, Horie Y, Faraon A. Decoupling optical function and geometrical form using conformal flexible dielectric metasurfaces. Nat Commun 2016;7:11618.
[82] Wu K, Coquet P, Wang QJ, Genevet P. Modelling of free-form conformal metasurfaces. Nat Commun 2018;9:3494.
[83] Teo JYH, Wong LJ, Molardi C, Genevet P. Controlling electromagnetic fields at boundaries of arbitrary geometries. Phys Rev A 2016;94:23820.
[84] Cheng J, Jafar-Zanjani S, Mosallaei H. All-dielectric ultrathin conformal metasurfaces: lensing and cloaking applications at 532 nm wavelength. Sci Rep-UK 2016;6:38440.
[85] Padgett M, Bowman R. Tweezers with a twist. Nat Photonics 2011;5:343–8.
[86] Wang J, Yang J, Fazal IM, et al. Terabit free-space data transmission employing orbital angular momentum multiplexing. Nat Photonics 2012;6:488–96.
[87] Mehmood MQ, Mei S, Hussain S, et al. Visible-frequency metasurface for structuring and spatially multiplexing optical vortices. Adv Mater 2016;28:2533.
[88] Huang L, Song X, Reineke B, et al. Volumetric generation of optical vortices with metasurfaces. ACS Photonics 2017;4:338–46.
[89] Tan H, Deng J, Zhao R, et al. A free-space orbital angular momentum multiplexing communication system based on a metasurface. Laser Photonics Rev 2019;13:1800278.
[90] Ahluwalia B, Yuan XC, Tao SH, et al. Microfabricated-composite-hologram-enabled multiple channel longitudinal optical guiding of microparticles in nondiffracting core of a Bessel beam array. Appl Phys Lett 2005;87:84104.
[91] Wang Z, Jiang L, Li X, et al. High-throughput microchannel fabrication in fused silica by temporally shaped femtosecond laser Bessel-beam–assisted chemical etching. Opt Lett 2018;43:98–101.
[92] Lin Z, Li X, Zhao R, et al. High-efficiency Bessel beam array generation by Huygens metasurfaces. Nanophotonics Berlin 2019;8:1079–85.
[93] Liu L, Zhang X, Kenney M, et al. Broadband metasurfaces with simultaneous control of phase and amplitude. Adv Mater 2014;26:5031–6.
[94] Lee G, Yoon G, Lee S, et al. Complete amplitude and phase control of light using broadband holographic metasurfaces. Nanoscale 2018;10:4237–45.
[95] Song X, Huang L, Tang C, et al. Selective diffraction with complex amplitude modulation by dielectric metasurfaces. Adv Opt Mater 2018;6:1701181.
[96] Song X, Huang L, Sun L, et al. Near-field plasmonic beam engineering with complex amplitude modulation based on metasurface. Appl Phys Lett 2018;112:73104.
[97] Zhao R, Huang L, Tang C, et al. Nanoscale polarization manipulation and encryption based on dielectric metasurfaces. Adv Opt Mater 2018;6:1800490.
[98] Overvig AC, Shrestha S, Malek SC, et al. Dielectric metasurfaces for complete and independent control of the optical amplitude and phase. Light Sci Appl 2019;8:1–12.
[99] Mo W, Wei X, Wang K, Li Y, Liu J. Ultrathin flexible terahertz polarization converter based on metasurfaces. Opt Express 2016;24:13621–7.
[100] Cong L, Xu N, Zhang W, Singh R. Polarization control in terahertz metasurfaces with the lowest order rotational symmetry. Adv Opt Mater 2015;3:1176–83.
[101] Zhang T, Huang L, Li X, Liu J, Wang Y. High-efficiency broadband polarization converter based on omega-shaped metasurface. J Phys D Appl Phys 2017;50:454001.
[102] Malek SC, Ee H, Agarwal R. Strain multiplexed metasurface holograms on a stretchable substrate. Nano Lett 2017;17:3641–5.
[103] Hwang C, Kim GH, Yang J, et al. Rewritable full-color computer-generated holograms based on color-selective diffractive optical components including phase-change materials. Nanoscale 2018;10:21648–55.
[104] Wang Q, Rogers ETF, Gholipour B, et al. Optically reconfigurable metasurfaces and photonic devices based on phase change materials. Nat Photonics 2016;10:60–75.
[105] Cheng Z, Rios C, Pernice WHP, Wright CD, Bhaskaran H. On-chip photonic synapse. Sci Adv 2017;3:e1700160.
[106] Zhu W, Yang R, Fan Y, et al. Controlling optical polarization conversion with Ge2Sb2Te5-based phase-change dielectric metamaterials. Nanoscale 2018;10:12054–61.
[107] Ji R, Hua Y, Chen K, et al. A switchable metalens based on active tri-layer metasurface. Plasmonics 2019;14:165–71.
[108] Li T, Huang L, Liu J, Wang Y, Zentgraf T. Tunable wave plate based on active plasmonic metasurfaces. Opt Express 2017;25:4216–26.
[109] Li T, Wei Q, Reineke B, et al. Reconfigurable metasurface hologram by utilizing addressable dynamic pixels. Opt Express 2019;27:21153–62.
[110] Choi C, Lee S, Mun S, et al. Metasurface with nanostructured Ge2Sb2Te5 as a platform for broadband-operating wavefront switch. Adv Opt Mater 2019;7:1900171.
[111] Lin Z, Huang L, Zhao R, et al. Dynamic control of mode modulation and spatial multiplexing using hybrid metasurfaces. Opt Express 2019;27:18740–50.
[112] Li J, Kamin S, Zheng G, et al. Addressable metasurfaces for dynamic holography and optical information encryption. Sci Adv 2018;4:r6768.
[113] Duan X, Liu N. Scanning plasmonic color display. ACS Nano 2018;12:8817–23.
[114] Dong K, Hong S, Deng Y, et al. A lithography-free and field-programmable photonic metacanvas. Adv Mater 2018;30:1703878.
[115] Li L, Cui TJ, Ji W, et al. Electromagnetic reprogrammable coding-metasurface holograms. Nat Commun 2017;8:197.
[116] Ye W, Zeuner F, Li X, et al. Spin and wavelength multiplexed nonlinear metasurface holography. Nat Commun 2016;7:11930.
[117] Almeida E, Bitton O, Prior Y. Nonlinear metamaterials for holography. Nat Commun 2016;7:12533.

[118] Reineke B, Sain B, Zhao R, et al. Silicon metasurfaces for third harmonic geometric phase manipulation and multiplexed holography. Nano Lett 2019;19:6585–91.
[119] Lin Z, Huang L, Xu ZT, et al. Four-wave mixing holographic multiplexing based on nonlinear metasurfaces. Adv Opt Mater 2019;1900782.
[120] Abdelwahab I, Grinblat G, Leng K, et al. Highly enhanced third-harmonic generation in 2D perovskites at excitonic resonances. ACS Nano 2018;12:644–50.
[121] Gao Y, Huang C, Hao C, et al. Lead halide perovskite nanostructures for dynamic color display. ACS Nano 2018;12:8847–54.
[122] Yue Z, Xue G, Liu J, Wang Y, Gu M. Nanometric holograms based on a topological insulator material. Nat Commun 2017;8:15354.
[123] Li X, Ren H, Chen X, et al. Athermally photoreduced graphene oxides for three-dimensional holographic images. Nat Commun 2015;6:6984.